Nonlocal electron electrodynamics in high-frequency capacitive discharges

H. C. Kim,[a] G. Y. Park, and J. K. Lee[b]
Department of Electronic and Electrical Engineering, Pohang University of Science and Technology, Pohang 790-784, Republic of Korea

(Received 7 November 2005; accepted 16 January 2006; published online 16 February 2006)

Several nonlocal electron behaviors in low-pressure high-frequency capacitive discharges were found through particle-in-cell/Monte Carlo simulations. First, a negative power deposition region becomes wider as the rf frequency decreases. Second, in the spatial profile of the amplitude of the rf electric field, a nonmonotonic structure appears at the bulk-sheath boundary along with an abrupt change in the phase of the rf electric field. Third, in the spatial profile of the amplitude of the rf electron current, the second peak appears in the bulk. © *2006 American Institute of Physics*. [DOI: 10.1063/1.2172353]

I. INTRODUCTION

In capacitively and inductively coupled rf discharges, nonlocal electron kinetics is the indispensable physics for a comprehensive understanding of low-pressure gas discharges.[1,2] In the presence of an ambipolar potential, the accessible volume of each electron depends on the energy. Therefore, low- and high-energy electrons should be considered separately. Low-energy electrons are trapped inside the potential well where the rf electric field is weak. Meanwhile, high-energy electrons can interact with the stronger rf field, where most of the power is deposited. An analogy can be made between the skin layer in an inductively coupled plasma (ICP) and the sheath in a capacitively coupled plasma (CCP). In an ICP, electrons gain energy in this strong field region and diffuse to the bulk of the plasma with the thermal velocity v_{th}. The distance these electrons travel during a rf period is on the order of v_{th}/f, where f is the rf frequency. The interaction of these traveling electrons with the inhomogeneous rf electric field outside the skin layer leads to several phenomena. These phenomena are associated with the so-called anomalous skin effect[3–5] and include negative power deposition, a nonmonotonic field profile, and a second current layer. Since the resonance particles with a velocity close to the phase velocity strongly interact with the rf field, they gain and lose energy in the regions of positive and negative power absorption, respectively.

Unlike the anomalous skin effect in ICPs, nonlocal electron electrodynamics in CCPs has been commonly understood by considering electrons as test particles, rather than the interaction between nonlocal energetic electrons and the rf field. Recently, Kaganovich[6] showed that there is a nonlinear interaction between electrons and an external rf field, even in CCPs, using a simple analytic model. Despite a few differences between ICPs and CCPs (such as the direction of the rf electric field to the wall and the importance of the ambipolar potential and magnetic field), some analogies can be made regarding the interaction between electrons and the rf field outside the skin layer or sheath.[7] Furthermore, in comparison to ICPs, diagnostics on the spatial profiles of the rf field and the electron current are limited in CCPs. Since the rf frequency determines the time scale for the interaction between electrons reflected from the sheath and the electric field in the bulk, it is particularly useful to see the effect of the rf frequency on the spatial profiles. Since very-high-frequency CCPs are becoming increasingly important for better performance in plasma processing, our work will be attractive not only for its physics but also for its applications.

In this paper, we report on several phenomena caused by the interaction between nonlocal energetic electron and the rf field outside the sheath. These phenomena include a region of negative power deposition as a function of the rf frequency, a nonmonotonic structure of the amplitude of rf electric field, and a second peak in the spatial profile of high-energy electron current.

II. PIC-MCC SIMULATION

In this study, to obtain the spatial profiles, we have used a one-dimensional electrostatic particle-in-cell (PIC) simulation method coupled with a Monte Carlo collision model (MCC).[8] This is self-consistent and fully kinetic. Our simulations were performed for argon discharges between two parallel-plate electrodes separated by a gap distance L of 3.5 cm. The ground state argon gas density is assumed to remain constant and uniform in space. The chemical reactions of atoms in excited states and Coulomb collisions between charged particles are not considered. Collisional effects are included by coupling the PIC method with the MCC technique.[9] For electrons colliding with neutrals, the elastic scattering, excitation, and ionization are taken into account. For argon ions colliding with neutrals, charge exchange and elastic scattering are considered. Another simulation result obtained by using this code shows a good agreement with experimental data.[10]

The gas pressure was set to 5 mTorr. At this pressure, electrons are nearly collisionless in their thermal motion. The discharge was driven by a rf current source applied to the powered electrode at position $x=0$. The electrode at position $x=L$ was grounded. To obtain the meaningful steady-state

[a]Also at the Department of Nuclear Engineering, University of California, Berkeley, California 94720-1730.
[b]Electronic mail: jkl@postech.ac.kr

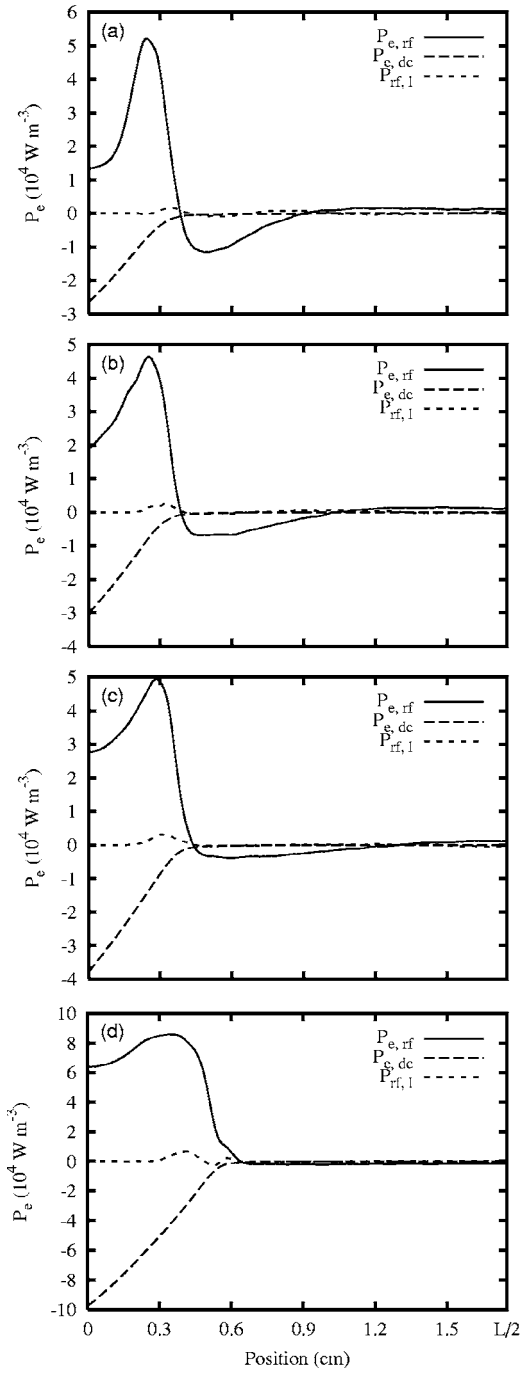

FIG. 1. Power deposition profiles at (a) 100, (b) 80, (c) 60, and (d) 40 MHz. Only the left-hand side of the system is plotted.

results, several thousand rf cycles were simulated for each run. For simplicity, the secondary electron emission was not taken into account in the simulation. The rf source current was fixed at 9 mA cm^{-2} and its frequency was varied from 40 to 100 MHz. Under the condition above, the rf frequency is much larger than the electron-neutral collision frequency and the plasma behaves inductively.[11]

III. RESULTS AND DISCUSSION

The spatial profiles of power deposited to the electrons at 100, 80, 60, and 40 MHz are shown in Fig. 1. They were time averaged over a rf period. Since the profile is symmetric to the discharge center, only the left-hand side of the profile is plotted. The total electron power $[P_e \equiv \langle J_e E \rangle]$ is divided into two components: dc power ($P_{e,\mathrm{dc}}$) and rf power ($P_{e,\mathrm{rf}}$). The dc power is defined as the power contributed from the dc electron current and the dc electric field $[P_{e,\mathrm{dc}} \equiv \langle J_e \rangle \langle E \rangle]$. Since the dc power is due to electron energy losses to the walls, it is negative in the sheath. As the rf frequency decreases, the increase in plasma potential leads to an increase of the negative dc power in the sheath. The rf power is defined as the power contributed from the sinusoidal electron current and the sinusoidal electric field. It is determined by the product of the magnitude of rf electron current ($J_{e,\mathrm{rf}}$), the magnitude of the rf electric field (E_{rf}), and the phase difference (ψ) between them:

$$P_{e,\mathrm{rf}} = J_{\mathrm{e,rf}} E_{\mathrm{rf}} \cos \psi. \tag{1}$$

The phase difference ψ determines the sign of the power deposition. When it is smaller than 90°, the power deposition is positive. Otherwise, it is negative.

As shown in Fig. 1, the rf power is positive in the sheath due to the sheath heating, but it is negative in a region that extends from the bulk-sheath boundary toward the discharge center. As the rf frequency decreases, the negative rf power deposition region becomes wider while its magnitude decreases. At 40 MHz, the rf power is negative in the whole bulk region, as shown in Fig. 1(d). The region of negative power deposition in a CCP can be explained in an analogy with an ICP, in terms of the excursion of energetic electrons from the sheath to the bulk. When these electrons reflected from the sheath return into the bulk, they gain energy from the dc field but lose energy from the rf field since rf power deposition is negative. Since the energy of the traveling electrons changes as they move, the excursion velocity v_x is not the same as the initial velocity but rather the mean velocity over their excursion distance. As the rf frequency decreases, the magnitude of the rf negative power deposition decreases and hence the excursion velocity v_x increases. Since the excursion time $(1/f)$ also increases, the excursion distance (v_x/f) increases. As a result, the negative power deposition region widens as the rf frequency decreases. For the case being studied, the length of this region becomes comparable to half the bulk length between 60 and 40 MHz.

The rf power contributed by low-energy electrons ($P_{\mathrm{rf},l}$) is also shown in Fig. 1. Since in our simulation the ambipolar potential is less than 3 eV, electrons with a total energy (the sum of kinetic and potential energies) lower than 3 eV are included in the low-energy electron group. The rf power contribution from low-energy electrons is quite small and the negative rf power deposition is therefore due to the collisionless cooling of nonlocal high-energy electrons (>3 eV).

When the electric field is assumed to be expressed as

$$E(t) = E_{\mathrm{dc}} + E_{\mathrm{rf}}, \tag{2}$$

$$= E_{\mathrm{dc}} + E_{\mathrm{rf0}} \cos(2\pi f t + \phi), \tag{3}$$

the dc electric field E_{dc} and the amplitude E_{rf0} and phase ϕ of the rf electric field can be obtained by the following formula:

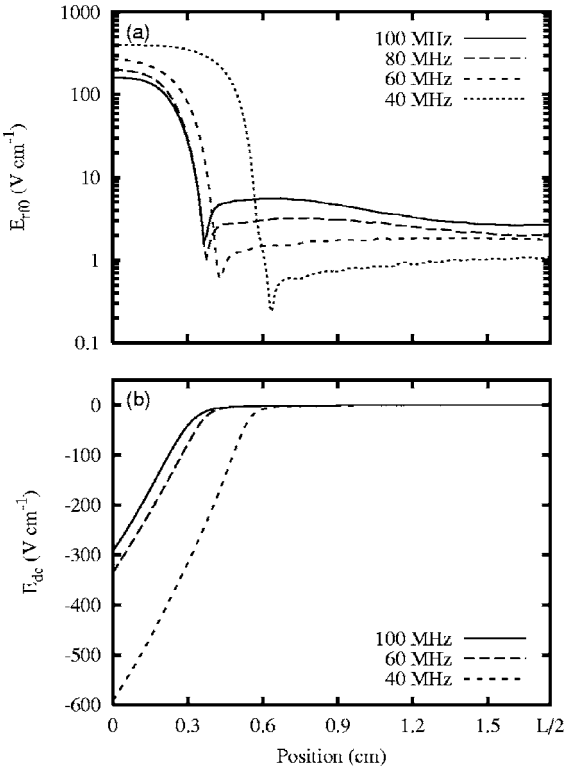

FIG. 2. The spatial profiles of (a) the rf electric field and (b) the dc electric field for different frequencies. Only the left-hand side of the system is plotted.

$$E_{\mathrm{dc}} = \langle E(t) \rangle, \tag{4}$$

$$E_{\mathrm{rf0}} = \sqrt{\langle 2E(t)\sin(2\pi ft)\rangle^2 + \langle 2E(t)\cos(2\pi ft)\rangle^2}, \tag{5}$$

and

$$\phi = \arctan\left(\frac{\langle E(t)\sin(2\pi ft)\rangle}{\langle E(t)\cos(2\pi ft)\rangle}\right), \tag{6}$$

where $\langle \cdot \rangle$ means averaging over the rf period. Figure 2(a) shows the spatial profiles of the rf electric field (E_{rf0}) for different frequencies. The rf field is large in the sheath and becomes small in the bulk. This is caused by the ion space charge screening in the sheath. The rapid decrease of the rf field from the wall to the bulk in a CCP is similar to that in the skin layer in an ICP, although they are based on different mechanisms. The profile of the dc field (E_{dc}) is monotonic, as shown in Fig. 2(b). In comparison, the rf field has a nonmonotonic structure at the bulk-sheath boundary, as shown in Fig. 2(a). Unlike the similar structure found in Refs. 12 and 13, this nonmonotonic structure appears, even when the Ramsauer minimum in the electron elastic collision cross section is not included. A similar nonmonotonic field structure was observed in an ICP by Godyak *et al.*[3] The nonmonotonic structure of the amplitude of the rf electric field is evidence of the nonlinear interaction of the rf electric field with energetic electrons. It cannot be explained in the model considering electrons as test particles.

The nonmonotonic structure of the amplitude of the rf electric field is different from the well-known field reversal.[14] The field reversal is related to different directions (or phases) of the rf field at the discharge center and the sheath. The nonmonotonic structure, however, is the spatially nonmonotonic amplitude of the rf field. As the rf frequency decreases, the plasma conductivity in low-pressure high-frequency CCPs increases. Hence, the rf field in the bulk decreases. As a result, the electron temperature for low-energy electrons at the discharge center decreases slightly (not shown here). The decrease of the rf field also results in the decrease of the magnitude of the negative rf power deposition, as shown in Fig. 1. On the other hand, as the rf frequency decreases, the rf field in the sheath increases due to the increase of the capacitive impedance.

Figure 3 shows the spatial profiles of the rf electron currents for different frequencies. The electron conduction current ($J_{e,\mathrm{rf0}}$) dominates in the bulk while the displacement current is dominant in the sheath. Because of the current continuity, the amplitude of the total rf electron current ($J_{e,\mathrm{rf0}}$) in the bulk is nearly the same as that of the applied current. The current continuity requires the total electron current perpendicular to the wall to be constant. However, the currents of low- and high-energy electrons having different kinetics can be spatially nonuniform.

The rf current contributions from low- ($J_{\mathrm{rf0},l}$) and high-energy electrons ($J_{\mathrm{rf0},h}$) are presented separately in Fig. 3. Two current peaks for the high-energy electrons appear at the bulk-sheath boundary and near the discharge center. The second current peak near the discharge center is formed by the electrons moved from the first peak. There is a local minimum point between the two current peaks. For 40 MHz, where the excursion distance is sufficiently larger than the bulk length, the two current peaks are not shown clearly. This is due to the significant mixing of the currents flowing from left and right sheaths. At this frequency, the rf power deposition is negative over the whole bulk region, as shown in Fig. 1(d). The region of negative rf power deposition is located between the position where the first current peak occurs and the local minimum current point (Figs. 1 and 3). The rf power deposition is positive between the local minimum point and the discharge center, except for the case of 40 MHz. The second peak in the high-energy electron current is located next to the region of negative rf power deposition. In comparison to an ICP, the low-energy electron current in the bulk is large in a CCP because the spatial length of the ambipolar field is comparable to that of the rf field.[7]

Figure 4 shows the spatial profiles of the phase of the rf electric field and the rf electron currents. They are calculated with respect to the phase of the applied current. The phase of the total electron current is zero in the bulk. At the bulk-sheath boundary, there is a field reversal point where the phase of the rf field changes abruptly. In a CCP, under the rf electric field with inhomogeneous amplitude and phase [Figs. 2(a) and 4], the resonant interaction of nonlocal energetic electrons with the electric field leads to the negative power profile, the nonmonotonic electric field structure, and the second peak in the high-energy electron current [Figs. 1, 2(a), and 3]. However, the reason for the spatial inhomogeneity in the phase of the rf field is different in CCPs and ICPs. In CCPs, the phase inhomogeneity is due to the ion space charge screening. On the other hand, in ICPs, the

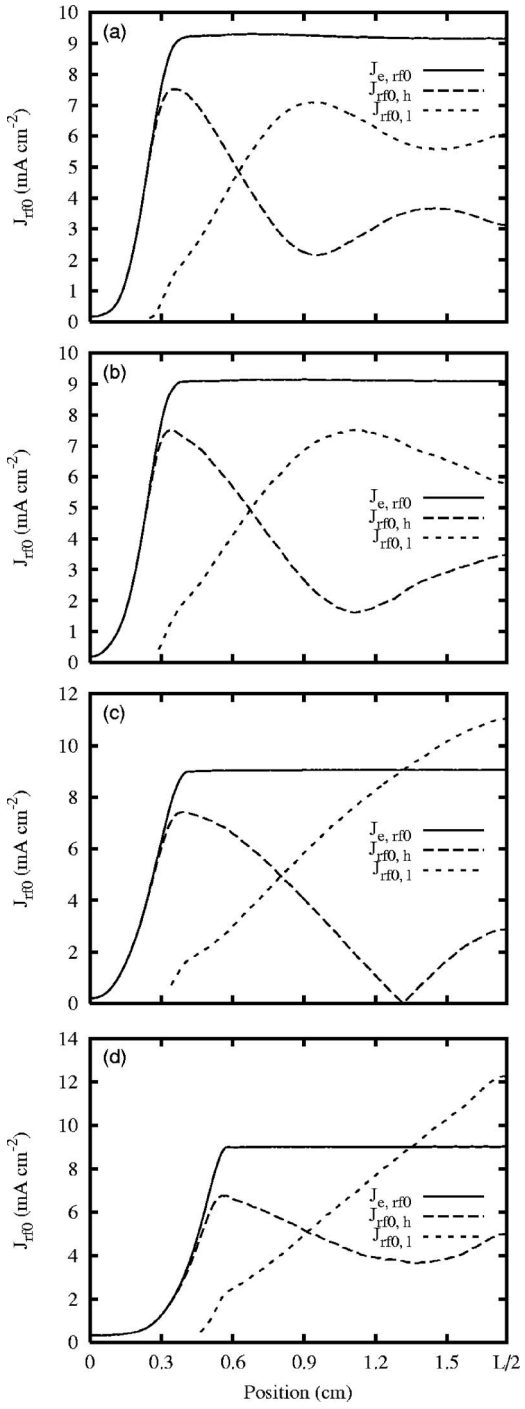

FIG. 3. The spatial profiles of the rf electron currents at (a) 100, (b) 80, (c) 60, and (d) 40 MHz. Only the left-hand side of the system is plotted.

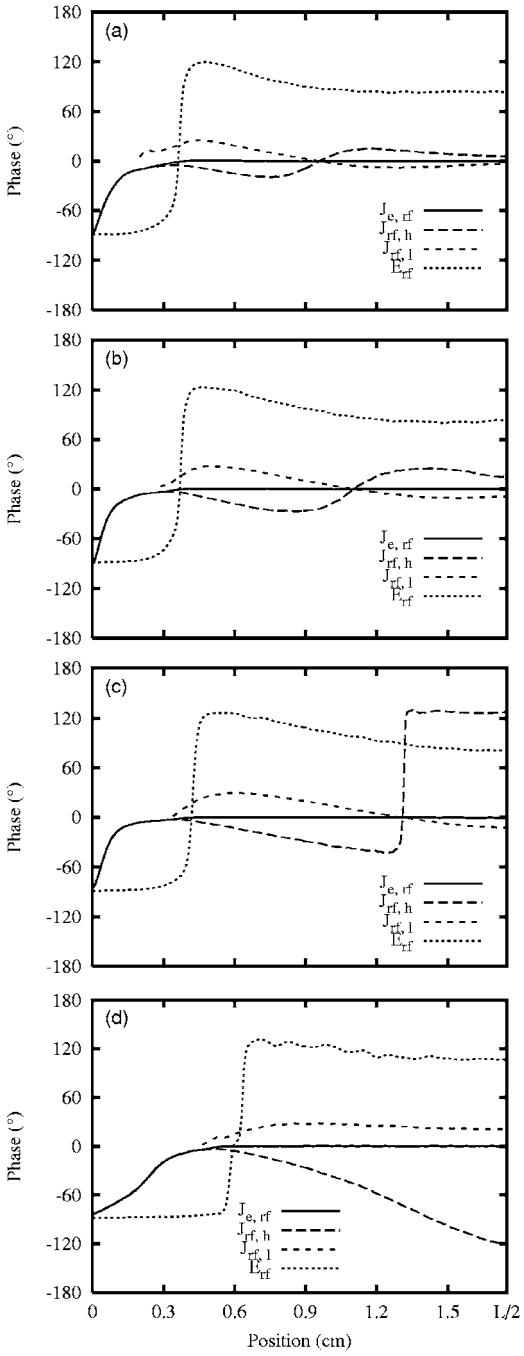

FIG. 4. The spatial profiles of the phase of the rf electric field and the rf electron currents at (a) 100, (b) 80, (c) 60, and (d) 40 MHz. They are calculated with respect to the phase of the applied current. Only the left-hand side of the system is plotted.

phase inhomogeneity is due to the significant electric field generated from the second current diffused from the skin layer. In CCPs, the electric field from the second current of the high-energy electrons is negligible compared to that from a large amount of low-energy electrons. Our result on the field phase profile is consistent with the result of Refs. 14 and 15 that the bulk electric field is largely out of phase with the sheath electric field.

High- and low-energy electron currents are out of phase with the total rf current in the bulk in Fig. 4. Low-energy electrons in the bulk are about 90° out of phase with the electric field. Thus its power deposition is negligible, as shown in Fig. 1. Except for the case of 40 MHz, there is a point in the bulk where the phases of low- and high-energy electron currents are zero. At this point, the phase of the high-energy electron current changes abruptly. Since the phase of the rf field is 90°, the rf power deposition is zero at that point.

IV. SUMMARY

Several nonlocal electron behaviors in low-pressure high-frequency capacitive discharges were found through PIC/MCC simulations. They originate from the interaction of

nonlocal energetic electrons with the rf electric field outside the sheath. A region of negative rf power deposition and a second current peak of the high-energy electron are formed when nonlocal energetic electrons reflected from the sheath return into the bulk. As the rf frequency decreases, the excursion distance of those electrons increases so that a wider negative power deposition region is created. In the spatial profile of the amplitude of the rf electric field, a nonmonotonic structure was obtained at the bulk-sheath boundary along with an abrupt change in the phase of the rf electric field.

ACKNOWLEDGMENTS

The helpful comments of Professor J. P. Verboncoeur at the University of California at Berkeley and Dr. F. Iza is greatly acknowledged. This work was supported in part by the Lam Research Corporation, Jusung Engineering, and Teralevel Nano Devices Project, 21c Frontier R&D Program in the Korea Ministry of Science and Technology.

[1] V. I. Kolobov and V. A. Godyak, IEEE Trans. Plasma Sci. **23**, 503 (1995).
[2] H. C. Kim, F. Iza, S. S. Yang, M. Radmilovic-Radjenovic, and J. K. Lee, J. Phys. D **38**, R283 (2005).
[3] V. A. Godyak, R. B. Piejak, and B. M. Alexandrovich, Phys. Plasmas **6**, 1804 (1999).
[4] V. A. Godyak, Phys. Plasmas **12**, 055501 (2005).
[5] V. I. Kolobov and D. J. Economou, Plasma Sources Sci. Technol. **6**, R1 (1997).
[6] I. D. Kaganovich, Phys. Rev. Lett. **89**, 265006 (2002).
[7] Y. M. Aliev, I. D. Kaganovich, and H. Schluter, Phys. Plasmas **4**, 2413 (1997).
[8] J. P. Verboncoeur, M. V. Alves, V. Vahedi, and C. K. Birdsall, J. Comput. Phys. **104**, 321 (1993).
[9] V. Vahedi and M. Surendra, Comput. Phys. Commun. **87**, 179 (1995).
[10] H. C. Kim, O. Manuilenko, and J. K. Lee, Jpn. J. Appl. Phys. **44**, 1957 (2005).
[11] M. A. Lieberman and A. J. Lichtenberg, *Principles of Plasma Discharges and Materials Processing* (Wiley, New York, 1994).
[12] H. C. Kim and J. K. Lee, Phys. Rev. Lett. **93**, 085003 (2004).
[13] H. C. Kim and J. K. Lee, Phys. Plasmas **12**, 053 501 (2005).
[14] T. J. Sommerer, W. N. G. Hitchon, and J. E. Lawler, Phys. Rev. Lett. **63**, 2361 (1989).
[15] M. Surendra and D. B. Graves, Phys. Rev. Lett. **66**, 1469 (1991).